



# An improved multi-objective particle swarm optimization using an efficient $G_{best}$ selection method

Yuki Hasegawa<sup>†</sup>, Takayuki Kimura<sup>‡</sup> and Kenya Jin'no<sup>‡</sup>

<sup>†</sup>Graduate School of Electronics, Information and Media Engineering, Nippon Institute of Technology  
4-1-1 Gakuendai, Miyasiro, Minami-Saitama, 345-8501, Japan

<sup>‡</sup>Department of Electrical and Electronic Engineering, Nippon Institute of Technology  
4-1-1 Gakuendai, Miyasiro, Minami-Saitama, 345-8501, Japan  
Email: hasegawa.2318@gmail.com, tkimura@nit.ac.jp, jinno@nit.ac.jp

**Abstract**—Accuracy, uniformity and breadth of Pareto-front are important indices for multi-objective optimization problems. However, the conventional multi-objective particle swarm optimization (MOPSO) considers only uniformity to construct the Pareto front. Although the MOPSO shows good performance on the low dimensional multi-objective optimization problems, it shows poor performance for the high dimensional ones. To overcome this problem, we have already improved the MOPSO using determination of initial positions of particles and an effective  $G_{best}$  selection method. In addition, we clarified that the improved method shows better performance than the original MOPSO for the benchmark problems. However, evaluations of our improved method for the real-world problems such as the hybrid renewable energy system is still remaining work. Thus, to investigate an applicable possibility of our improved method for the real-world optimization problems, we evaluate the improved method using the hybrid renewable energy system in this study.

## 1. Introduction

An optimization problem that tries to solve multiple objectives simultaneously is called a multi-objective optimization problem. Generally, the multi-objective optimization problem is defined as follows:

$$\begin{aligned} f(\mathbf{x}) &= (f_1(\mathbf{x}), \dots, f_m(\mathbf{x}))^T, \\ \mathbf{x} &= (x_1, \dots, x_n)^T. \end{aligned} \quad (1)$$

In Eq. (1),  $f(\mathbf{x})$  is the  $m$  dimensional objective functions and  $\mathbf{x}$  is  $n$  dimensional variables. As one of the efficient methods for solving the multi-objective optimization problems, the multi-objective particle swarm optimization(MOPSO) has already been proposed[1]. Although this method shows good performance on low dimensional multi-objective benchmark problems, its performance is degraded on the high dimensional ones. To overcome this problem, determination of initial positions of particles and an effective  $G_{best}$  selection method are applied to MOPSO in Ref.[2]. In addition, we clarified that the improved method shows better performance than the MOPSO for the benchmark problems. However, evaluations of improved method for the real-world problems such as the hybrid renewable energy system(HRES)[3] is still remaining

work. Thus, we evaluate the improved method using the HRES in this study to investigate the applicable possibility of our improved method for the real-world optimization problems. From the numerical experiments, the improved method shows good performance for rated value decision problems in the HRES.

## 2. Multi-Objective Particle Swarm Optimization (MOPSO)

In the MOPSO[1],  $\mathbf{x}_k(i)$  is the position of the  $i$  th particle at the  $k$  th iteration, and  $\mathbf{v}_k(i)$  is the velocity of the  $i$  th particle at the  $k$  th iteration. Then, to find the optimum Pareto-front, the MOPSO algorithm works as follows:

### step 1 : Initialization of the particles

The initial position of the  $i$  th particle,  $\mathbf{x}_0(i)$ , is randomly determined. In addition, the initial velocity of the  $i$  th particle,  $\mathbf{v}_0(i)$ , is set to 0.

### step 2 : Updating the $\mathbf{P}_{best}(i)$ and $\mathbf{G}_{best}$

$\mathbf{P}_{best}(i)$  is the position of the  $i$  th particle where the best evaluation value was obtained in the past searching history.  $\mathbf{G}_{best}$  is the position of the particle when the best evaluation value were obtained among all the particles. In the searching process of the MOPSO, if a non-dominated solution is obtained, this solution is stored in the archiving space.  $\mathbf{P}_{best}(i)$  is updated if the  $i$  th particle finds the best evaluation value. In addition,  $\mathbf{G}_{best}$  is also updated if the particle finds the best value during the searching history.

### step 3 : Formation of the hypercube

The solution space is divided to form the hypercubes. The hypercube is used to measure the density of the solutions in the solution space.

### step 4 : Selection of the global best

To select the global best used in MOPSO, the evaluation value for the hypercube that expresses the density of the solutions in the solution space is defined as follows:

$$D_i = \begin{cases} \frac{rand(0,1)}{H_i} & \text{(if a solution exists in the } i \text{ th hypercube),} \\ 0 & \text{(otherwise).} \end{cases} \quad (2)$$

In Eq. (2),  $D_i$  is the density of the solutions in the  $i$  th hypercube and  $H_i$  is the number of solutions in the  $i$  th hypercube. If Eq. (2) takes large value, or the small number of solutions exist in a hypercube, one of the solutions in the hypercube is selected as the next global best.

**step 5** : Updating the velocity and position of the particles  $v_{k+1}(i)$  and  $x_{k+1}(i)$  are updating as follows:

$$v_{k+1}(i) = \omega v_k(i) + rand_1 C_1 (P_{best}(i) - x_k(i)) + rand_2 C_2 (G_{best} - x_k(i)), \quad (3)$$

$$x_{k+1}(i) = x_k(i) + v_{k+1}(i). \quad (4)$$

In Eq. (3),  $\omega$  is the inertia weight,  $rand_1$  and  $rand_2$  are the uniformly distributed random numbers within the range of  $[0, 1]$ , and  $C_1$  and  $C_2$  are the acceleration weights.

**step 6** : Evaluation of the particles

Calculation of the objective function is finally conducted using the current position of the particles.

Steps 2 to 6 are repeated until the termination condition is satisfied.

### 3. Our improved method using determination of initial positions of particles and an effective $G_{best}$ selection method[2]

In this section, we described an improved MOPSO method[2].

#### 3.1. Determination of initial position of particle

To eliminate the possibility for getting into the local minima by the MOPSO, we add the determination method for the initial positions of particles[4] into the conventional MOPSO (DP-MOPSO). In the DP-MOPSO, the searching process of the optimum Pareto front is divided into two stages. In the first stage, the optimum points in the solution space are obtained using the single PSO (Fig. 1(a)). Obtained positions of the particles are stored in the archiving space. In addition, the searching process of the optimum point for each objective function is performed in the second stage, and the obtained positions are also stored in the archiving space. Next, the MOPSO starts searching the optimum Pareto front using the particles whose initial positions are set to the ones in the archiving space. The initial positions of the particles are randomly selected from the ones stored in the archiving space. Schematic diagram for the determination method of initial positions of particles in the DP-MOPSO is described in Fig.1.

#### 3.2. An effective $G_{best}$ selection method

In the conventional MOPSO, the ununiform Pareto front is obtained because the global best  $G_{best}$  that determines the directions of all the particles using Eq. (2). We

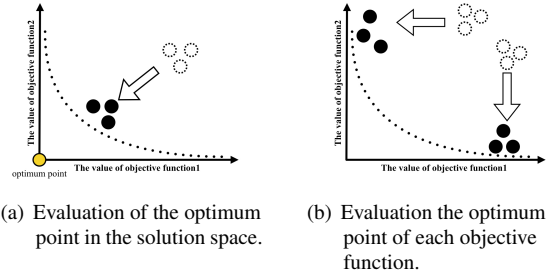


Figure 1: Determination of initial position of particles

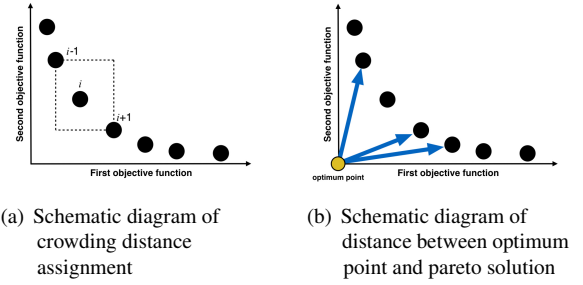


Figure 2: An effective  $G_{best}$  selection method

then change this global best selection method using improved crowding-distance-assignment. By using the improved crowding-distance-assignment, the solution that is the closest to the optimum solution is easily selected as the  $G_{best}$  at each iteration. The improved crowding-distance-assignment of the  $i$  th non-dominated solution is defined as follows:

$$CD_i = \frac{1}{EUC(ND_i, Opt)} \frac{ND_{i+1} - ND_{i-1}}{f_{max} - f_{min}} \quad (5)$$

In Eq. (5),  $EUC(ND_i, Opt)$  is an euclidean distance between the optimum point  $Opt$  and the  $i$  th non-dominated solution  $ND_i$ ,  $f_{max}$  and  $f_{min}$  is the maximum and minimum values of the objective functions. Schematic diagram of the effective  $G_{best}$  selection method is described in Figs.2.

### 4. Hybrid Renewable Energy System(HRES)

A HRES[3] is a power supply system integrating the renewable energy systems to reduce the unpredictability of the power by the renewable energies (Fig. 3). In the HRES, the output power to meet the demand of the consumer is mainly produced by the photovoltaic power generation system and the wind turbine. If the output power is greater than the power demand, surplus electric power will be stored in the battery. In addition, if the charging electric power for the battery meets the maximum capacity, remaining power will be used to extract the hydrogen from  $H_2O$ , then, the hydrogen is charged into the hydrogen tank. If the output power from the photovoltaic system and the wind turbine cannot meet the energy demand, the saving power by the battery and the hydrogen tank will be used to supply the shortage power. Further, if the power from the

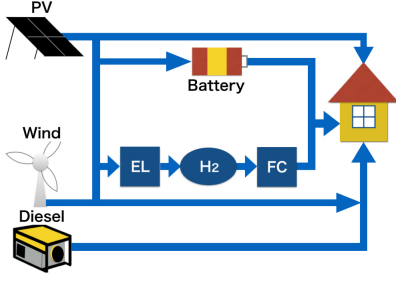


Figure 3: Configuration of the hybrid renewable energy systems.

photovoltaic system, the wind turbine, the battery and the hydrogen tank can not meet the demand, the diesel generator starts to supply the power demand as the backup power, then, the CO<sub>2</sub> emission from the HRES increases.

The rated power of the system  $P$  is defined as follow:

$$P = [P_{PV}, P_{WG}, P_{bat}, P_{EL}, P_{tank}, P_{FC}, P_{Dis}], \quad (6)$$

where  $P_{PV}$ [kW] is the rated power of the photovoltaic power generation system,  $P_{WG}$ [kW] is the rated power of the wind turbine power generation system,  $P_{bat}$ [kW] is the rated capacity of the battery,  $P_{EL}$ [kW] is the rated capacity of the electrolytic cell,  $P_{tank}$ [kg] is the rated capacity of the hydrogen tank,  $P_{FC}$ [kW] is the rated power of the fuel cell, and  $P_{Dis}$ [kW] is the rated power of the diesel generator.

Mathematical model of each system is discribed as follows:

- Wind turbine power generation system:

Output power from the wind turbine power generation system,  $E_{WG}$ , is defined as follows:

$$E_{WG} = \begin{cases} 0 & v \leq V_c, \\ P_{WG} \frac{v - V_c}{V_r - V_c}^3 & V_c \leq v < V_r, \\ P_{WG} & V_r \leq v < V_f, \\ 0 & v \geq V_f, \end{cases} \quad (7)$$

where  $V_c$  is the cut-in wind speed,  $V_r$  is the rated wind speed,  $V_f$  is the cut-out wind speed, and  $P_{WG}$  is the rated power of the wind turbine.

- Photovoltaic power generation system:

Output power from the photovoltaic power generation system,  $E_{PV}$ , is defined as follows:

$$E_{PV} = \eta_{PV} p_v P_{PV}, \quad (8)$$

where  $p_v$  is the radiation of sunlight,  $P_{PV}$  is the rated power of the PV panel, and  $\eta_{PV}$  is the conversion efficiency.

- Electrolyzer:

The amount of hydrogen  $Q_{H2}$  is defined as follows:

$$Q_{H2} = \frac{E_{EL}}{\alpha_E \eta_{EL}}, \quad (9)$$

where  $E_{EL}$  is the power consumption of the electrolyzer,  $\alpha_E$  is a coefficient of power consumption curve, and  $\eta_{EL}$  is the electrolysis efficiency.

- Fuel cell:

The fuel cell is used as a backup generator by converting electrical energy into chemical energy of hydrogen and an oxidant. Consumption of hydrogen in the fuel cell  $H_{2cons-FC}$  is defined by,

$$H_{2cons-FC} = \alpha_{FC} P_{a-FC} \eta_{FC}, \quad (10)$$

where  $P_{a-FC}$  is the output power of fuel cell,  $\alpha_{FC}$  is a coefficient of hydrogen consumption curve, and  $\eta_{FC}$  is a power generation efficiency.

- Diesel generator:

The diesel generator is used as an emergency power source. The fuel consumption of the diesel generator,  $fuel_{cons}$ , is defined by,

$$fuel_{cons} = \alpha_{DG} P_{a-DG} \eta_{DG}, \quad (11)$$

where  $P_{a-DG}$  is the output power of the diesel generator,  $\alpha_{DG}$  is a coefficient of fuel consumption curve, and  $\eta_{DG}$  is a power generation efficiency.

- Battery:

The state of charge at the  $t$ th time of the battery,  $SOC(t)$  is defined by,

$$SOC(t) = \begin{cases} SOC(t-1) + \left(\frac{E_{bat}(t)\eta_{charge}}{P_{bat}}\right) \times 100 & (charging), \\ SOC(t-1) - \left(\frac{E_{bat}(t)\eta_{discharge}}{P_{bat}}\right) \times 100 & (discharging), \end{cases} \quad (12)$$

$$SOC_{min} \leq SOC(t) \leq SOC_{max}, \quad (13)$$

where  $E_{bat}$  is the amount of power charging or discharging the battery,  $P_{bat}$  is the rated capacity of the battery,  $\eta_{charge}$  is a charging efficiency,  $\eta_{discharge}$  is a discharging efficiency. The battery can discharge the energy until the power reaches  $SOC_{min}$ , and charges until it reaches  $SOC_{max}$ .

- Hydrogen tank:

The amount of the the hydrogen at the  $t$ th time,  $H_{2level}(t)$ , is define by,

$$H_{2level}(t) = H_{2(t-1)} + Q_{H2}(t) - \frac{H_{2cons-FC}(t)}{\eta_{H2-tank}}, \quad (14)$$

$$H_{2levelmin} \leq H_{2level}(t) \leq H_{2levelmax}, \quad (15)$$

where  $Q_{H_2}$  is the mass flow rate of hydrogen electrolyzer,  $H_{2cons-FC}(t)$  is the hydrogen consumption of the fuel cell, and  $\eta_{H_2-tank}$  is the storing efficiency.

Also, the hydrogen tank has an upper limit and a lower limit to storage the hydrogen. The upper limit of the hydrogen tank,  $H_{2levelmax}$ , is defined by the rated capacity of hydrogen, and the lower limit,  $H_{2levelmin}$ , is defined by 5% of the rated capacity of the hydrogen tank.

To determinate the optimum rated value of the HRES, we consider the following objectives, 1) the amount of the CO<sub>2</sub> emission, and 2) the total cost of the system. The total cost includes the initial cost, the operation, maintenance costs, the replacement cost, and fuel costs. Each objective for the HRES is defined as follows:

- The amount of the CO<sub>2</sub> emission

The amount of the CO<sub>2</sub> emission is defined by,

$$CO_{2emission} = \sum_{t=1}^{8760} fuel_{cons}(t) \times EF, \quad (16)$$

where  $EF$  is the emission factor of diesel generator. We set the cost of the EF €1.2 for 2.5[kg/lt].

- Total cost of the system

The total cost of the system is defined as follows:

$$cost = \sum_j [C_{I,j} + C_{OM,j} \frac{1}{CRF(i,T)} + C_{rep,j} K_j] P_j + C_{IS,j} + C_{OMS,j} + C_{fuel} \times fuel_{cons,yr} \times \frac{1}{CRF(i,T)}, \quad (17)$$

$$K_j = \sum_{n=1}^Y \frac{1}{(1+i)^{L \times n}}, \quad (18)$$

$$Y = \begin{cases} \frac{T}{L} - 1 & T\%L = 0, \\ \frac{T}{L} & T\%L \neq 0, \end{cases} \quad (19)$$

$$CRF = \frac{ir(1+ir)^T}{(1+ir)^T - 1}, \quad (20)$$

where  $C_{I,j}$  is the investment cost of the component  $j$ ,  $C_{OM,j}$  is the operation and the maintenance cost of the component  $j$ ,  $C_{rep,j}$  is the replacement cost of the component  $j$ ,  $C_{fuel}$  is fuel costs,  $fuel_{cons,yr}$  is the fuel consumption by lt/yr annual,  $C_{IS,j}$  is the intercept of the investment cost of the component  $j$ ,  $C_{OMS,j}$  is the intercept of the operation and maintenance cost of the component  $j$ ,  $K_j$  is the worth of the single payment,  $CRF$  is the capital recovery factor, represented in Eqs. (18), (19) and (20), respectively. In Eqs. (18), (19) and (20),  $ir$  is interest rates,  $L$  and  $Y$  are life time and the number of replacement of the component  $j$ ,  $T$  is 25-year project life.

## 5. Numerical experiments

In these numerical experiments, we compared the performance of the IC-DPMOPSO with that of the conventional MOPSO for the rated value decision problems. We set the number of iterations to 1,000, the number of particles to 200. Results of the Pareto solution set obtained by the conventional MOPSO and IC-DCMOPSO for the rated value decision problem of HRES are shown in Fig. 4. In Fig. 4, pareto solution set by the IC-DPMOPSO shows better uniformity than that by the conventional MOPSO.

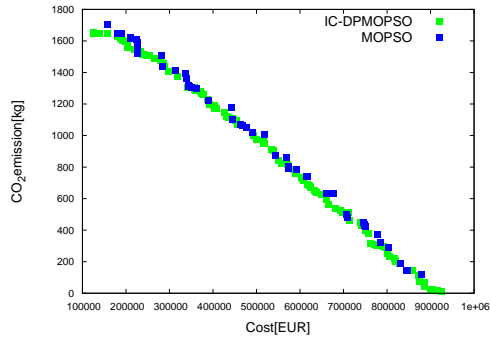


Figure 4: Pareto solution set obtained by the conventional MOPSO and IC-DCMOPSO

## 6. Conclusion

In this study, we evaluated the improved MOPSO[2] for the rated value decision problem of HRES to investigate the applicable possibility of our improved method for the real-world optimization problems. From the results of the numerical experiments, we confirmed the improvement of uniformity and breadth of the pareto front can be obtained by the improved method. In the future work, we propose a better solution method as compared to improved method[2] for the other real multi objective optimization problems.

The research of T.K. was partially supported by a Grant-in-Aid for Young Scientists (B) from JSPS (No.16K21327).

## References

- [1] C. A. Coello Coello and M. S. Lechuge, *IEEE International Conference on Evolutionary Computation*, Vol. 2, pp. 1051-1056, 2002.
- [2] Yuki Hasegawa, Takayuki Kimura and Kenya Jin'no, *Proc. 2016 RISP International Workshop*, pp. 221-224, 2016.
- [3] M. Sharafi and T. Y. ElMekkawy, *Renewable Energy*, Vol. 68, pp. 68-79, 2014.
- [4] Masashi Nishioka, Tomoyuki Hiroyasu, Mitsunori Miki and Hisatake Yokouchi, *The Japan Society of Mechanical Engineers*, Vol. 5361, pp. 219-224, 2008.